Quality Assurance and Safety of Crops & Foods, 2018; 10 (4): 371-381

The effect of short and medium infrared radiation on some drying and quality characteristics of quince slices under vacuum condition

B. Alaei[1], N. Dibagar[1], R. Amiri Chayjan[1*], M. Kaveh[2] and E. Taghinezhad[3]

[1]Department of Biosystems Engineering, Faculty of Agriculture, Bu-Ali Sina University, Hamedan, Iran; [2]Department of Biosystems Engineering, Faculty of Agriculture and Natural Resources, University of Mohaghegh Ardabili, 59661-14477 Ardabil, Iran; [3]Moghan College of Agriculture and Natural Resources, University of Mohaghegh Ardabili, 56199-11367 Ardabil, Iran; amirireza@basu.ac.ir, amirichayjan@gmail.com

Received: 25 July 2017 / Accepted: 2 August 2018

RESEARCH ARTICLE

Abstract

Infrared assisted vacuum drying technology is a newly emerged strategy, which found its place in the food drying industry. Therefore, in this research, the effectiveness of near infrared (NIR) and medium infrared (MIR) radiation was experimentally investigated on drying kinetics and some quality properties of quince slices under vacuum condition. Experiments were conducted at drying temperatures of 50, 60 and 70 °C and absolute pressures of 20, 40 and 60 kPa for NIR and MIR radiations. Drying process in MIR assisted vacuum drying domain lasted about 3 to 28 min lower than NIR one, indicating improved drying process under MIR condition. Effective moisture diffusivity for NIR domain was obtained in the range of 0.17×10^{-9} to 0.46×10^{-9} m^2/s while it was between 0.18×10^{-9} to 0.46×10^{-9} m^2/s under MIR condition. Minimum specific energy consumption for NIR and MIR radiation was estimated 0.55 and 0.34 kWh, respectively. Total colour difference and sample shrinkage under NIR radiation were calculated within the range of 5.5 to 25.4% and 40.4 to 64.5%, respectively, which were significantly lower the ranges of MIR. Minimum total colour change (5.5%) and shrinkage (40.4%) of quince samples were calculated under NIR condition while, the minimum values for MIR domain were 12.1 and 50%, respectively.

Keywords: drying characteristics, infrared dryer, vacuum condition, quince quality

1. Introduction

Quince fruit (*Cydonia oblonga*), one of the exclusive members of genus *Cydonia* in the family *Rosaceae*, is well known for its individual characteristics such as delicious taste and pleasant odour (Doymaz *et al.*, 2015; Ziaforoughi *et al.*, 2016). Apple and pear are the other members of this family. The quince fruit is a good source of minerals such as magnesium, copper, iron, potassium and vitamin C followed by B-complex vitamins (Magalhaes *et al.*, 2009). It was claimed that quince is a low-cost product while it is a rich source of phenolic acids and flavonoids (Dehghannya *et al.*, 2018; Silva *et al.*, 2004, 2008). Based on the report of statistic centre, annual world production of quince in 2012 was 596,532 tons (FAO, 2014). In the last few years, Iran consistently has been among the top countries producing quince in the world. Turkey, Morocco, Argentina, China, Uzbekistan and Azerbaijan are the other major producers. Fresh quince consumption is difficult due to its astringent and sour taste. Hence, its consumption after drying, cooking or processing as juices, pies, jam or jelly, marmalade, and candies are more popular. Dried quince slices can be utilised as an ingredient in traditional Iranian food such as quince stew and chowder (Noshad *et al.*, 2012).

Drying is a one of the beneficial post-harvest preservation methods to extend the shelf life of the agricultural products by minimising microbiological and water activities of dried product. Due to the lighter weight, dried agricultural materials can be stored infinitely and transported easily. Even though the drying process is a most frequent strategy employed in the food stability improvement, this is a complex method involves simultaneous heat and mass transfer. The theoretical application of food drying becomes difficult due to the physical and chemical changes occur in the complex structure of the biological material during drying. For this reason, many attempts have been made by thousands of researchers to analyse the final physical quality of different fruits and vegetables after drying process such as terebinth (Kaveh *et al.*, 2015), Yacon (Shi *et al.*, 2014), apple (El-Mesery and Mwithiga, 2015), shiitake mushroom (Wang *et al.*, 2015), hawthorn (Aral and Bese, 2016) and apple (Beigi, 2016).

Cost-effective and sanitary preservation methods have significant importance in product drying. Application of various types of modern dryers decreases the material losses and increases the product quality as compared to traditional methods, including sun and shade drying (Akpinar *et al.*, 2003). The use of radiant power in the drying industry has gained momentum due to its intrinsic superiorities rather than conventional drying techniques. These benefits include progress in radiator construction, fast response time, significant energy saving, acquired space, product uniform temperature, superior thermal efficiency, quality preservation and high heat transfer coefficient (Wang and Sheng, 2006). Radiant power is employed to eliminate moisture with radiation, which penetrates to the materials, but penetration power is limited (Ginzburg, 1969). The penetration depth depends on the infrared radiation (IR) wavelengths, the structure and composition of the fruits. When a radiation penetrates to the food materials, caused a severe heating and reduced the temperature gradient in material within shorter drying time (Atungulu and Pan, 2011). IR waves comprise three categories of near infrared (NIR), medium infrared (MIR) and far infrared (FIR). NIR has the short length waves ranging from 750 to 2,000 nm, while MIR has the medium length waves in the range of 2,500 to 4,000 nm (Antal *et al.*, 2017; Chablani *et al.*, 2011). FIR consists of long length waves of 4 to 100 μm (Reich, 2005). IR is transferred through water at shortwave length, while, it is absorbed on the surface at long wavelength (Sakai and Hanzawa, 1994). Hence, drying of thin layer products find to be more effective at FIR, nevertheless drying of thicker bio-products gives better results when it is exposed to the NIR (Alaei and Amiri Chayjan, 2015b). In other words, penetration depth of the FIR energy is very low, while penetration depth of NIR energy varied from 1 to 18 mm for different agricultural products (Krishnamurthy *et al.*, 2008).

Combined drying techniques are including of the several drying methods and have many benefits over other purely drying methods. (Huang *et al.*, 2015). Recently, infrared assisted vacuum drying of fruits, vegetables and grains has been investigated as a potential technique to produces high quality dried food products. An infrared vacuum dryer offers an efficient system taking the advantages of fast mass transfer, low temperature and more porous microstructure from vacuum and rapid energy transfer from infrared heating. Various products were subjected to infrared vacuum drying process such as pumpkin slices (Ghaboos *et al.*, 2016), miang leaves (Hirun *et al.*, 2015) and pomegranate arils (Alaei and Amiri Chayjan, 2015a). So, many researches have been reported for agricultural materials drying using IR-vacuum dryer.

According to our knowledge, no research has been reported about the effect of different infrared waves on quality properties of quince slices under vacuum condition. Therefore, this research was undertaken to investigate the effect of near and medium infrared waves on drying properties (effective moisture diffusivity; D_{eff} and specific energy consumption; SEC) and some quality characteristics (shrinkage and total colour change) of quince slices under a vacuum condition.

2. Materials and methods

Preparation of quince slices

Fresh quince fruit was purchased from a local market. After cleaning and washing, the quince was cut into the samples of 3 mm thickness then they were cut into cylindrical shape by a ring cutter with an inner diameter of 28 mm. The weight of each sample was about 38±5 g and a single layer containing 12 slices was placed on the tray for each trail. Samples were subjected to the drying temperatures of 50, 60 and 70 °C and absolute pressures of 20, 40 and 60 kPa. Experiments were conducted in triplicates. Initial moisture content (MC) of quince was calculated 5.21% (dry basis) using an oven (Memmert INB200, Memmert GmbH + Co. KG, Schwabach, Germany) at 70 °C for 24 h (AOAC, 2002). The samples were dried to reach final MC of 0.1% (d.b.). During the experiments, the lab ambient air temperature and relative humidity were in the range between 22 to 30 °C and 20 to 30%, respectively.

Experimental setup

Supplementary Figure S1 shows a lab scale infrared assisted vacuum dryer, which was manufactured in the Department of Biosystems Engineering, University of Bu-Ali Sina, Hamedan, Iran. The drying chamber was constructed using a hollow Teflon cylinder. A tungsten lamp (100 W) and a quartz lamp (100 W) were applied as a thermal source of NIR and MIR radiation on top of the drying chamber. They provided necessary heat and radiant power for drying process. The distance between the lamp and samples tray was about 5 cm. A vacuum pump (DV, 285N, 250 Platinum, JB Industries, Inc., Aurora, IL, USA) was connected to the chamber through high-pressure pipes to create the vacuum conditions in drying chamber. The electrical control system consists of a thermostat (Atbin 400k, Atbin Co., Tehran, Iran) and a pressure controller (Sensys PSCH0001 BCIJ, Sensor System Technology Co., Ltd, Gyeonggi-Do, South Korea). Thermostat and pressure controller are able to control the temperature inside the chamber and the absolute pressure during drying (0.001 bar accuracy), respectively. The MC of samples was measured periodically using a digital scale (AND, GF-6000, A&D Company Ltd, Tokyo, Japan) with accuracy 0.01 g every five minutes until to reach the safe level of 0.1% (d.b.).

Drying kinetics

MC of quince sample was calculated during drying process as follows (Kaveh *et al.*, 2018):

$$MC = \frac{(W_t - W)}{W_t} \quad (1)$$

where, MC is the moisture content (g water/g dry matter), W_t is the total weight of quince (g) and W is the weight of quince after drying (g) (Eltawil *et al.*, 2018).

Moisture ratio (MR) of quince fruit during drying was computed utilising Equation 2 (Kaveh *et al.*, 2017):

$$MR = \frac{(M - M_e)}{(M_0 - M_e)} \quad (2)$$

Where, MR is the moisture ratio, M is the MC at time t (g water/g dry matter), M_o and M_e are the initial and equilibrium MC (d.b.), respectively. In each temperature and relative humidity, the equilibrium MC (M_e) of the samples is relatively small as compared to M or M_o, therefore M_e was numerically set to zero in this research. So $(M–M_e)$ / $(M_o–M_e)$ can be simplified as follows (Calin-Sanchez *et al.*, 2014):

$$MR = \frac{M}{M_0} \quad (3)$$

Effective moisture diffusivity

Fick's second law of diffusion is expressed as the following equation to describe the moisture diffusion process in a spherical shape (Castro and Pinheiro, 2016).

$$\frac{\partial M}{\partial t} = D_{eff} \nabla^2 M \quad (4)$$

Where D_{eff} is the effective moisture diffusivity (m^2/s), t is the drying time (s) and M is the MC (d.b.). Regarding the slab shape of quince slices, following assumptions were considered (Caglar *et al.*, 2009): (1) moisture distribution in the mass is uniform; (3) mass transfer is symmetric according to centre; (3) surface MC of the samples immediately reaches equilibrium in the ambient air; (4) resistance to the mass transfer is negligible compared to the internal resistance and e) diffusion coefficient is fixed and shrinkage is negligible. Based on these assumptions, the D_{eff} can be obtained from the following equation (Kaveh and Amiri Chayjan, 2017):

$$MR = \frac{M - M_e}{M_o - M_e} = \frac{8}{\pi^2} \sum_{n=1}^{\infty} \frac{1}{(2n+1)} \exp\left(\frac{-D_{eff}(2n+1)^2 \pi^2 t}{4L^2} \right) \quad (5)$$

Where n is the drying terms (1, 2, 3,...) and L is the half of the slab thickness of quince (m), M_o is the initial MC (d.b.) and M_e is the equilibrium MC (d.b.) and is considered to be zero. When t increases, all sentences are zero except the first. Therefore, the above equation can be simplified as Equation 6 (Demiray and Tulek, 2017):

$$MR = \frac{M}{M_o} = \frac{8}{\pi^2} \exp\left(-\frac{\pi^2 D_{eff} t}{4L^2} \right) \quad (6)$$

After linearisation:

$$\ln(MR) = Ln(\frac{M}{M_o}) = \ln(\frac{8}{\pi^2}) - \left(\frac{\pi^2 D_{eff} t}{4L^2} \right) \quad (7)$$

Plotting ln(MR) versus time would result in a line with slope k, D_{eff} can be calculated as follows:

$$k = \left(\frac{D_{eff} \pi^2}{4L^2} \right) \quad (8)$$

Specific energy consumption

SEC of NIR/MIR vacuum dryer was equal to the sum of energy required for vacuum pump and NIR and MIR lamp. *SEC* of vacuum pump can be determined using Equation 9 (Motevali *et al.*, 2011). The vacuum pump power in the set up was 380 W.

$$SEC_1 = P_1 \times t_1 \quad (9)$$

Where SEC_1 is the energy consumption of vacuum pump (kWh), P_1 is the pump nominal power (kW) and t_1 is the working time of pump (h). The energy requirement of NIR and MIR lamps of power 100 W were constant during drying and was calculated using Equation 10 (Motevali *et al.*, 2011).

$$SEC_2 = P_2 \times t_2 \quad (10)$$

Where, SEC_2 is the energy consumed by *NIR* lamp (kWh), P_2 is the lamp nominal power (kW) and t_2 is a total operating time of lamp during drying of quince slices (h). Total SEC for the hybrid *NIR* or MIR vacuum dryer was evaluated as follows (Alaei and Amiri Chayjan, 2015a):

$$EC_T = EC_1 + EC_2 \quad (11)$$

Colour

According to the contradiction of commercial instruments for colour measurement and due to their only application in engineering researches, this research renders a simple indirect method that uses a flatbed scanner to measure colour and the graphics software Photoshop to analyse colour. The term 'measure' means that the flatbed scanner

(HP Scanjet G4050 Photo Scanner, HP Inc., Palo Alto, CA, USA) was used to obtain the colour values of the pixels on the quince slices surface. The term 'analyse' means that Photoshop was employed to manipulate those colour values to achieve colour distribution, averages, and so on. Similar applications of this indirect procedure were reported in colour measurements of paddy (Golpour *et al.*, 2015) and pumpkin (Ghaboos *et al.*, 2016). All surfaces were scanned using a flatbed scanner with a resolution of 1,200 dpi (Sorouraddin *et al.*, 2005).

The scanned images were transferred to Photoshop CS6 software (CBS Interactive Inc., San Francisco, CA, USA) and the colour parameters of *L* (brightness), *a* (green (-a) to red (+a)) and *b* (blue (-b) to yellow (+b)) obtained. Using the following formulas *L, a,* and *b* converted to L^* (whiteness/darkness), a^* (redness/greenness), b^* (yellowness/blueness) parameters (Alaei and Amiri Chayjan, 2015a).

$$L^* = \frac{L}{255} \times 100 \tag{12}$$

$$a^* = \frac{240a}{255} - 120 \tag{13}$$

$$b^* = \frac{240b}{255} - 120 \tag{14}$$

The total colour difference (ΔE) was then calculated using the following equation (Cheng *et al.*, 2015):

$$\Delta E = \sqrt{\left(L^*_0 - L^*_t\right)^2 + \left(a^*_0 - a^*_t\right)^2 + \left(b^*_0 - b^*_t\right)^2} \tag{15}$$

Shrinkage

Shrinkage is volume changes of the biological materials due to water evaporation during drying process. Based on the measuring of primary and secondary volumes of material, shrinkage ratio (S_b) was calculated using the following formula (Paengkanya *et al.*, 2015; Zielinska *et al.*, 2015).

$$S_b(\%) = \left(\frac{V_0 - V}{V_0}\right) \times 100 \tag{16}$$

Where, V_0 is the initial or primary volume of the sample (m^3) and V is the secondary or final volume of the sample after drying (m^3). The volume of sample was calculated using the toluene displacement method (Mohsenin, 1986).

Experimental uncertainty

The analysis of uncertainties in experimental measurement is a powerful tool, particularly when it is used in the planning and design of experiments. Uncertainties analyses are given with Equation 17 (Beigi *et al.*, 2017; Horuz *et al.*, 2017):

$$W = \left[\left(\frac{\partial F}{\partial x_1} W_1\right)^2 + \left(\frac{\partial F}{\partial x_2} W_2\right)^2 + \ldots + \left(\frac{\partial F}{\partial x_n} U_n\right)^2 \right]^{0.5} \tag{17}$$

During measurement and calculation of the parameters, the involved uncertainties were determined and presented in Table 1

3. Results and discussion

Drying kinetics

The experimental data on the near and medium infrared assisted vacuum drying of quince slices in terms of typical diagrams of MC versus drying temperature and absolute pressure are shown in Figures 1 and 2, respectively. It is obvious that for all drying conditions, the MC value of quince fruit exponentially decreased during drying. According to the experimental results, drying temperature and absolute pressure affected the drying time under both NIR and MIR conditions. High temperatures assisted with lower absolute pressures led to a rapid quince MC reduction. In other word, drying process improved significantly when drying process adjusted with the highest temperature and lowest absolute pressure. This phenomenon is due to the high penetration of radiation energy to the material in the high temperature and low pressure. It was found that drying temperature was more effective on drying time as compared to chamber pressure. It is attributed to the increase in temperature gradient between product and its surroundings as well as increase in heat transfer and moisture diffusivity. In addition, when increasing radiation intensities, heater surface temperature increase, as well and lead to increase in material temperature however, MC decreases. The

Table 1. Uncertainties in the parameters measurement during drying experiment.

Parameter	Unit	Uncertainty
Inlet temperature in convective dryer	°C	±0.2
Outlet temperature in convective dryer	°C	±0.2
Ambient air temperature	°C	±0.2
Drying cabinet inlet temperature	°C	±0.2
Drying cabinet outlet temperature	°C	±0.2
Uncertainty in the measurement of relative humidity of air	RH	±0.1
Uncertainty in the measurement of moisture quantity	g	±0.001
Uncertainty in the absolute pressures	kPa	±0.8
Moisture diffusivity	%	±0.1-0.2
Uncertainty in the quartz lamp	W	±0.5
Uncertainty in the tungsten lamp	W	±0.5
Drying time measurement	s	±0.14
Mass loss measurement	g	±0.45

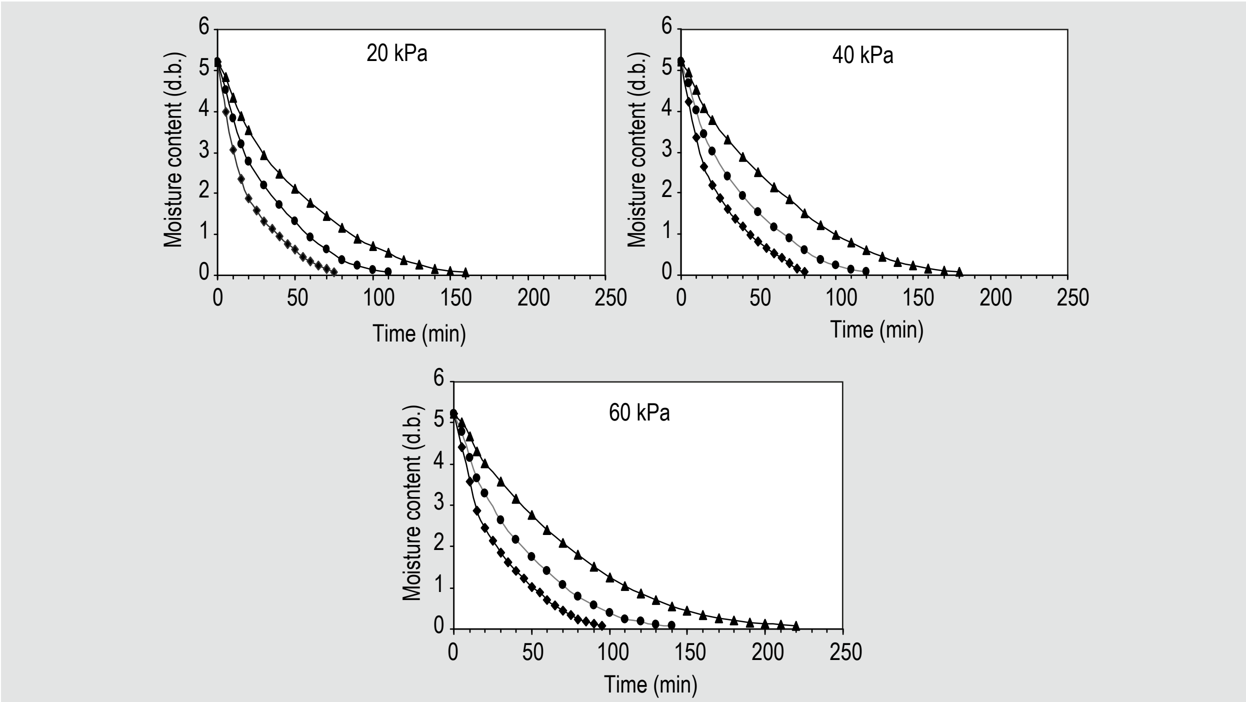

Figure 1. Effect of drying temperature on moisture content of quince slice in near infrared (NIR) assisted vacuum drying domain.

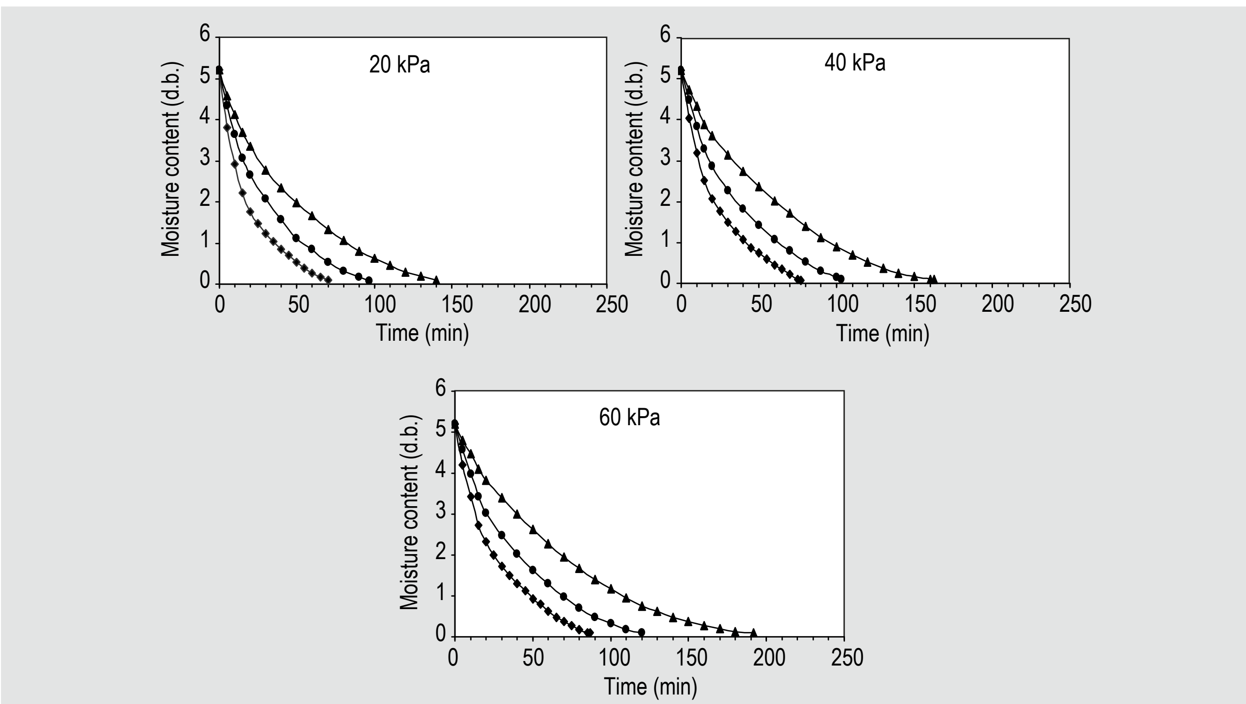

Figure 2. Effect of drying temperature on moisture content of quince slice in medium infrared (MIR) assisted vacuum drying domain.

maximum time lasted to reach the final MC of 0.1% (d.b.) in quince slices was 220 min and belonged to the drying temperature of 50 °C and absolute pressure of 60 kPa under NIR condition. However, minimum drying time (70 min) was related to the 70 °C and 20 kPa under MIR condition indicating that MIR accompanied by vacuum condition yields a rapid drying process. These results are in good agreement with the previous researches, such as: shiitake mushroom (Kantrong *et al.*, 2014), pomegranate (Alaei and Amiri Chayjan, 2015a), flos lonicerae (Liu *et al.*, 2015) and pumpkin slices (Ghaboos *et al.*, 2016). Effect of medium wave infrared on drying time was more pronounced rather than NIR under similar drying conditions. The drying time under NIR and MIR conditions varied between 3 to 28 min. The reason for this phenomenon could be due to the different absorption of IR wavelengths by quince slices and the various radiation patterns in the quartz and tungsten lamps.

Effective moisture diffusivity

The D_{eff} of quince fruit was computed using the procedure of slopes. D_{eff} is typically determined by drawing experimental drying data in terms of the natural logarithm of MC against time (as given in Equation 8). Under both NIR and MIR conditions, the D_{eff} in a thin layer of quince slices was influenced by independent variables namely drying temperature and absolute pressure. According to diffusivity values listed in Table 2 and Table 3, a nonlinear association was found between D_{eff} and independent variable of drying temperature and chamber absolute pressure. D_{eff} values of quince slices were within the range of 0.17×10^{-9} to 0.44×10^{-9} m^2/s and 0.18×10^{-9} to 0.46×10^{-9} m^2/s under near and medium wave infrared, respectively. These variation ranges are in agreement with D_{eff} values reported for food materials under infrared drying, which is reported between 10^{-12} to 10^{-8} m^2/s (Chen *et al.*, 2017; Jahedi Rad *et al.*, 2018; Kaveh *et al.*, 2018; Kocabiyik *et al.*, 2016; Onwude *et al.*, 2018). Due to the rapid water movement at high temperatures, D_{eff} values rose with an increase in process temperature and decrease in absolute pressure (Doymaz, 2014; Ghaboos *et al.*, 2016). When samples were exposed to the high process temperatures, heating energy increased and consequently caused increase in activity of water molecules and D_{eff}, as well (Ah-Hen *et al.*, 2013). Based on key results, maximum values of D_{eff} were obtained for NIR (0.44×10^{-9} m^2/s) and MIR (0.46×10^{-9} m^2/s) conditions under drying temperature of 70 °C, and vacuum pressure of 20 kPa. While the minimum D_{eff} values (0.17×10^{-9} and 0.18×10^{-9} for NIR and MIR conditions, respectively) belonged to the temperature of 50 °C and vacuum pressure of 60 kPa. D_{eff} increased with increase in drying temperature and vacuum pressure reduction. Comparatively, D_{eff} of quince slices under MIR was more than NIR at the same drying conditions, for this reason, the drying rate in MIR was higher than NIR domain. These values are comparable with other infrared-vacuum dried products such as pumpkin slices with D_{eff} range of 0.71×10^{-9} m^2/s (Ghaboos *et al.*, 2016) and pomegranate arils in the range of 3.07×10^{-10} to 1.14×10^{-9} m^2/s (Alaei and Amiri Chayjan, 2015a).

Specific energy consumption

Total SEC was calculated using Equation 11. The values of SEC versus drying temperature and absolute pressure are shown in Figures 3 and 4 (NIR and MIR domains). The SEC value of dried samples was achieved within the ranges of 0.55 to 0.85 kWh and 0.34 to 0.72 kWh for NIR and MIR domains, respectively. The maximum value of SEC (0.85 kWh for NIR and 0.72 kWh for MIR conditions) was obtained at the absolute pressure of 20 kPa and temperature of 50 °C. SEC decreased with temperature and vacuum pressure increment, because the working time of NIR or MIR lamp and vacuum pump were decreased. The similar results had been reported in drying of pomegranate arils

Table 2. Effective moisture diffusivity (D_{eff}) values of quince slices at various drying conditions in near infrared vacuum drying condition.

Air temperature	20 kPa		40 kPa		60 kPa	
(°C)	(m^2/s)D_{eff}	R^2	(m^2/s)D_{eff}	R^2	(m^2/s)D_{eff}	R^2
50	0.22×10^{-9}	0.9723	0.20×10^{-9}	0.9703	0.17×10^{-9}	0.9859
60	0.32×10^{-9}	0.9806	0.29×10^{-9}	0.9721	0.26×10^{-9}	0.9825
70	0.44×10^{-9}	0.9705	0.40×10^{-9}	0.9558	0.36×10^{-9}	0.9718

Table 3. Effective moisture diffusivity (D_{eff}) values of quince slices at various drying conditions in medium infrared (MIR) vacuum drying condition.

Air temperature	20 kPa		40 kPa		60 kPa	
(°C)	(m^2/s)D_{eff}	R^2	(m^2/s)D_{eff}	R^2	(m^2/s)D_{eff}	R^2
50	0.23×10^{-9}	0.9595	0.21×10^{-9}	0.9579	0.18×10^{-9}	0.9696
60	0.35×10^{-9}	0.9612	0.31×10^{-9}	0.9521	0.27×10^{-9}	0.9633
70	0.46×10^{-9}	0.9720	0.43×10^{-9}	0.9558	0.38×10^{-9}	0.9631

under vacuum conditions (Motevali *et al.*, 2011) and drying of nectarine slices under the near-infrared-vacuum conditions (Alaei and Amiri Chayjan, 2015b).

Colour

The colour preservation of biological products is considered as a quality indicator to assess the level of deterioration due to thermal processing (Doymaz and Altiner, 2012; Horuz and Maskan, 2015). In the marketing, the colour value is a major concern affecting product acceptance by consumers. The effect of drying temperature and absolute pressure on ΔE coefficient is depicted in Figures 5 and 6 for near and medium wave infrared, respectively. ΔE determines the quantity of colour change in dried samples with respect to the colour of fresh quince. Accordingly, the minimum ΔE value represents the high quality of dehydrated bio-product (Kantrong *et al.*, 2014). Variation ranges of ΔE for quince slices were from 5.5 to 16.7 and from 12.1 to 25.4 under NIR and MIR conditions, respectively. The results (Figure 5 and 6) showed that fewer colour differences were obtained in quince samples for low drying temperature, and absolute pressure. Therefore, both parameters (drying temperature and vacuum pressure) influenced ΔE. A number of chemical reactions were found to occur under drying process of biological materials. One of them is the Maillard reaction (Chen *et al.*, 2015), known to be responsible for non-enzymatic browning. Furthermore, degradation process of pigment was increased at the high temperatures.

Salarikia *et al.* (2017) reported that the temperature of 30 °C was the most effective temperature led to ΔE reduction in peppermint leaves under different drying methods. In addition, Alaei and Amiri Chayjan (2015a) reported lower colour changes for pomegranate arils with a decrease in air temperature and an increase in absolute pressure. Other similar results were found in Sumic *et al.* (2017) for mushroom using infrared-vacuum drying and Jafarifar *et al.* (2017) for walnut kernel subjecting to different drying methods with microwave pretreatment. The ΔE values of quince slices under NIR condition were low as compared to MIR condition. Because, the pigments might be less destroyed and the natural colour was more preserved (Kantrong *et al.*, 2014). Therefore, the quality loss can be reduced by using the combined NIR vacuum strategies. It is attributed to the fact that total ΔE could be affected by the uniform heat of incandescent bulbs and decreased Maillard reaction during drying process under shortwave IR.

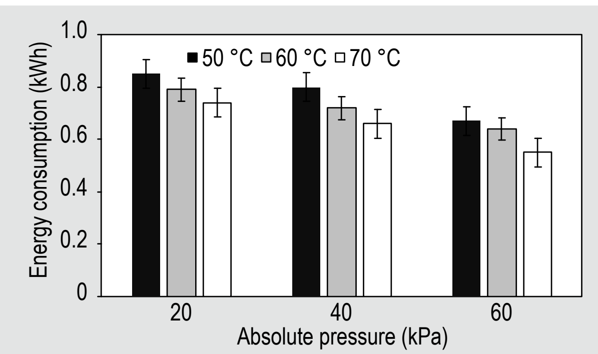

Figure 3. Plot of total specific energy consumption versus drying temperature and absolute pressure under in medium infrared (MIR) assisted vacuum drying domain.

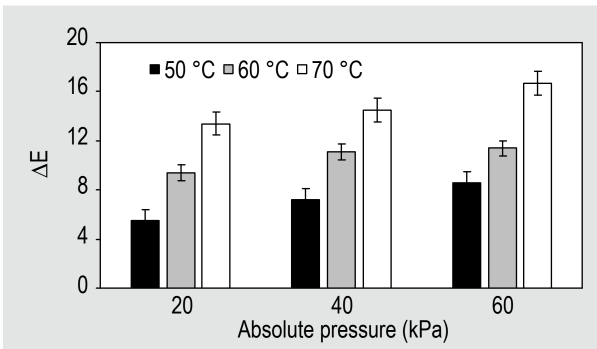

Figure 5. Plot of total colour change versus drying temperature and absolute pressure in near infrared (NIR) assisted vacuum drying domain.

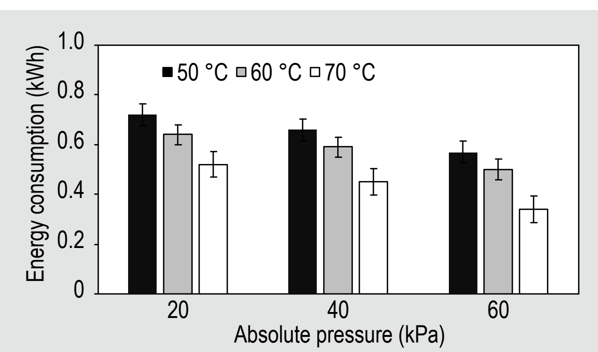

Figure 4. Plot of total specific energy consumption versus drying temperature and absolute pressure in medium infrared (MIR) assisted vacuum drying domain.

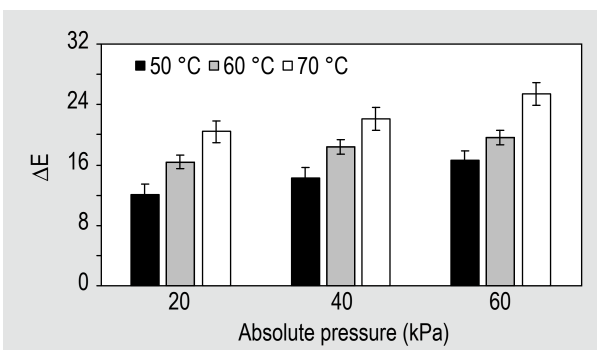

Figure 6. Plot of total colour versus drying temperature and absolute pressure in medium infrared (MIR) assisted vacuum drying domain.

Shrinkage

Shrinkage of quince slices took place during the drying process in NIR/MIR assisted vacuum drying domain. The plot of shrinkage percentage against process temperature and absolute pressure under short and medium wave IR is illustrated in Figure 7 and 8, respectively. The shrinkage coefficient of quince slices during drying was relatively low as compared to many foodstuffs due to their high MC such as fruits and vegetables. The final shrinkage percentage of the quince fruit ranged from 40.4 to 55.3% and 50 to 64.5% under NIR and MIR conditions, respectively. While shrinkage values of fruit and vegetable were reported between 70 to 90% (Alaei and Amiri Chayjan, 2015a). Minimum shrinkage (40.4 and 50% for NIR and MIR conditions, respectively) was obtained at drying temperature of 50 °C and vacuum pressure of 20 kPa. The temperature of 70 °C and the pressure of 60 kPa yielded the maximum shrinkage (55.3 and 64.5% for NIR and MIR conditions, respectively). Longer drying time of quince slices under NIR condition caused a uniform distribution of heat on samples, which is an effective factor on the reduction of shrinkage percentage. As shown in Figure 7 and 8, the highest shrinkage value was calculated at the highest temperature (70 °C) and absolute pressure (60 kPa) level. This is due to the faster mass transfer, so the created free space causes a tension in the quince tissue and then product became more wrinkled. When water is removed from a foodstuff, a pressure unbalance is generated between the inner of the material and the external pressure. This creates the contracting stresses that lead to material shrinkage or collapse. As a result, product shape changes and occasionally leads to cracking of the product. This is also the reason why vacuum drying, leads in general too much less shrinkage (Kurozawa *et al.*, 2012). Similar results have been reported for papaya (Kurozawa *et al.*, 2012), pineapple (Ponkham *et al.*, 2012) and terebinth fruit (Kaveh *et al.*, 2015). Also, the shrinkage coefficient values of quince slices under shortwave IR were lower than medium wave IR. At final, from the physical point of view, the NIR dried quince slices had the most similarity to that fresh one (Figure 9).

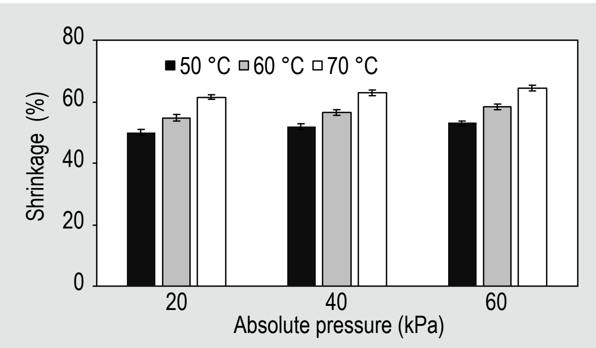

Figure 7. Plot of shrinkage versus drying temperature and absolute pressure in near infrared (NIR) assisted vacuum drying domain.

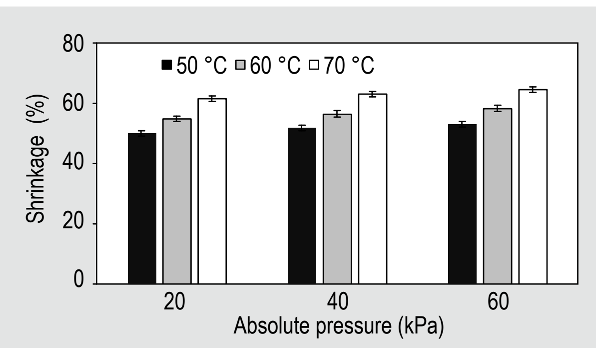

Figure 8. Plot of shrinkage versus drying temperature and absolute pressure in medium infrared (MIR) assisted vacuum drying domain.

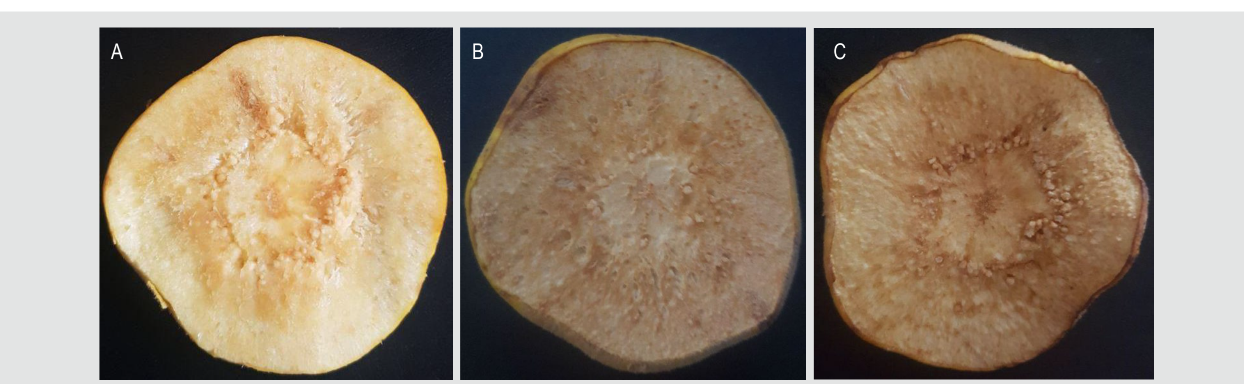

Figure 9. The image of the quince slices under various drying conditions, (A) control sample (before drying), (B) the minimum ΔE and shrinkage value in air temperature (50 °C), absolute pressure (20 kPa) under near infrared wave and (C) the highest ΔE and shrinkage value in air temperature (70 °C), absolute pressure (60 kPa) under medium infrared wave.

Table 4. Analysis of variance (ANOVA) table for the effect of process parameters undergoing NIR/MIR (near infrared/medium infrared) assisted vacuum drying.

		NIR		MIR	
Sources changes	DF	Mean of square	F-value	Mean of square	F-value[1]
Specific energy consumption (kWh)					
A (absolute pressures)	2	0.0688	294.86**	0.0562	337.40**
B (air temperature)	2	0.0343	147.00**	0.1057	634.40 *
A × B	4	0.0006	2.79 *	0.0003	2.00*
Colour					
A (absolute pressures)	2	17.67	478.29**	40.39	2,423.40**
B (air temperature)	2	136.09	3,683.64**	155.37	9,322.20**
A × B	4	0.76	20.57*	1.01	60.90*
Shrinkage					
A (absolute pressures)	2	33.28	1,109.33**	22.583	1,355.00**
B (air temperature)	2	279.01	9,300.33**	294.173	17,650.4**
A × B	4	0.56	18.67*	0.098	5.90*

[1] ** Significant at the 1% level; * significant at 5%.

Statistical analysis

Experimental data were statistically analysed using IBM SPSS Statistics 20 (IBM Corporation, Armonk, NY, USA). Analysis of variance (ANOVA) showed that drying temperature and absolute pressure had significant effect on the SEC, total colour change and shrinkage at probability level of 0.01 (Table 4). In addition, the interaction effect of absolute pressures and drying temperature was also significant on the SEC, total colour and shrinkage values (P<0.05).

4. Conclusions

Drying specifications of quince slices were investigated in a novel prototype of near and medium infrared-vacuum dryer under temperature and vacuum pressure levels of 50-70 °C and 20-60 kPa, respectively. Drying time of quince slices decreased with increasing drying temperature and decreasing absolute pressure under both NIR and MIR conditions. Drying time under MIR was about 3 to 28 min lower than near infrared condition. Effective moisture diffusivity of samples under medium wave infrared at different drying conditions (0.18×10^{-9} to 0.46×10^{-9} m^2/s) was more than near infrared values (0.17×10^{-9} to 0.44×10^{-9} m^2/s). SEC values for NIR and MIR obtained in the range of 0.55-0.85 and 0.34-0.72 kWh, respectively. Total colour change and sample shrinkage under shortwave infrared at different drying conditions were within the range of 5.5 to 25.4 and 40.4% to 64.5%, respectively, which were less than medium wave infrared values. Combined MIR radiation with vacuum operation economically is preferred to NIR radiation since it consumed less energy due to shorter drying time however; in terms of quality, the performance of NIR radiation under vacuum condition was much better.

Supplementary material

Supplementary material can be found online at https://doi.org/10.3920/QAS2017.1252

Figure S1. Schematic of infrared-vacuum dryer.

References

Ah-Hen, K., Zambra, C.E., Aguero, J.E., Vega-Galvez, A. and Lemus-Mondaca, R., 2013. Moisture diffusivity coefficient and convective drying modelling of murta (Ugni molinae Turcz): influence of temperature and vacuum on drying kinetics. Food and Bioprocess Technology 6: 919-930.

Akpinar, E.K., Biecr, Y. and Yildiz, C., 2003. Thin layer drying of red pepper. Journal of Food Engineering 59: 99-104.

Alaei, B. and Amiri Chayjan, R., 2015a. Drying characteristics of pomegranate arils under near infrared-vacuum conditions. Journal of Food Processing and Preservation 39: 469-479.

Alaei, B. and Amiri Chayjan, R., 2015b. Modelling of nectarine drying under near infrared-vaccum conditions. Acta Scientiarum Polonorum. Technologia Alimentaria 14: 15-27.

Antal, T., Tarek, M., Tarek-Tilistyák, J. and Kerekes, B., 2017. Comparative effects of three different drying methods on drying kinetics and quality of Jerusalem Artichoke (*Helianthus tuberosus* L.). Journal of Food Processing and Preservation 41(3): e12971.

Association of Official Analytical Chemists (AOAC), 2002. Official methods of analysis. Method number 934.06. AOAC, Arlington, VA, USA.

Aral, S. and Bese, A.V., 2016. Convective drying of hawthorn fruit (Crataegus spp.): effect of experimental parameters on drying kinetics, color, shrinkage, and rehydration capacity. Food Chemistry 210: 577-584.

Atungulu, G.G. and Pan, Z., 2011. Infrared radiative properties of food materials. Processing. CRC Press, Boca Raton, FL, USA.

Beigi, M., 2016. Hot air drying of apple slices: dehydration characteristics and quality assessment. Heat and Mass Transfer 52: 1435-1442.

Beigi, M., Torki-Harchegani, M. and Tohidi, M., 2017. Experimental and ANN modeling investigations of energy traits for rough rice drying. Energy 141: 2196-2205.

Caglar, A., Togrul, I.T. and Togrul, H., 2009. Moisture and thermal diffusivity of seedless grape under infrared drying. Food and Bioproduct Processing 87: 292-300.

Calin-Sanchez, A., Figiel, A., Wojdylo, A., Szaryez, M. and Carbonell-Barrachina, A.A., 2014. Drying of garlic slices using convective pre-drying and vacuum-microwave finishing drying: kinetics, energy consumption, and quality studies. Food and Bioprocess Technology 7: 398-408.

Castro, L.M.M.N. and Pinheiro, M.N.C., 2016. A simple data processing approach for drying kinetics experiments. Chemical Engineering and Communication 203: 258-269.

Chablani, L., Taylor, M.K., Mehrotra, A., Rameas, P. and Stagner, W.C., 2011. Inline real-time near-infrared granule moisture measurements of a continuous granulation – drying-milling process. AAPS Pharmaceutical Science and Technology 12: 1050-1055.

Chen, Q., Bi, J., Wu, X., Yi, J., Zhou, L. and Zhou, Y., 2015. Drying kinetics and quality attributes of jujube (Zizyphus jujube Miller) slices dried by hot air and short- and medium-wave infrared radiation. LWT – Food Science and Technology 64: 759-766.

Chen, Q., Bi, J., Chen, R., Liu, X., Wu, X. and Zhou, M., 2017. Comparative study on drying characteristic, moisture diffusivity, and some physical and nutritional attributes of blanched carrot slices. Journal of Food Processing and Preservation 41(5): e13201.

Cheng, L., Fang, S. and Ruan, M., 2015. Influence of blanching pretreatment on the drying characteristics of cherry tomato and mathematical modeling. International Journal of Food Engineering 11: 265-274.

Dehghannya, J., Hosseinlar, S.H. and Heshmati, M.K., 2018. Multi-stage continuous and intermittent microwave drying of quince fruit coupled with osmotic dehydration and low temperature hot air drying. Innovative Food Science and Emerging Technologies 45: 132-151.

Demiray, E. and Tulek, Y., 2017. The effect of pretreatments on air drying characteristics of persimmons. Heat and Mass Transfer 53: 99-106.

Doymaz, I., Demir, H. and Yildirim, A., 2015. Drying of quince slices: effect of pretreatments on drying and rehydration characteristics. Chemical Engineering Communications 202(10): 1271-1279.

Doymaz, I., 2014. Suitability of thin-layer drying models for infrared drying of peach slices. Journal of Food Processing and Preservation 38: 2232-2239.

Doymaz, I. and Altiner, P., 2012. Effect of pretreatment solution on drying and color characteristics of seedless grapes. Food Science and Biotechnology 21: 43-49.

El-Mesery, H.S. and Mwithiga, G., 2015. Performance of a convective, infrared and combined infrared-convective heated conveyor-belt dryer. Journal of Food Science and Technology 52: 2721-2730.

Eltawil, M.A., Azam, M.M. and Alghannam, A.O., 2018. Solar PV powered mixed-mode tunnel dryer for drying potato chips. Renewable Energy 116: 594-605.

Food and Agriculture Organisation (FAO), 2014. Food and population: FAO looks ahead. FAO, Rome, Italy.

Ghaboos, S.H.H., Ardabili, S.M.S., Kashaninejad, M., Asadi, G. and Aalami, M., 2016. Combined infrared-vacuum drying of pumpkin slices. Journal of Food Science and Technology 53: 2380-2388.

Ginzburg, A.S., 1969. Application of radiation in food processing. Leonard Hill Books, London, UK.

Golpour, I., Amiri Chayjan, R., Amiri Parian, J. and Khazaei, J., 2015. Prediction of paddy moisture content during thin layer drying using machine vision and artificial neural networks. Journal of Agricultural Science and Technology 17: 287-298.

Hirun, S., Choi, J.H., Ayarungsaritkul, J., Pawsaut, C., Sutthiwanjampa, C., Vuong, Q.V., Chockchaisawasdee, S., Heo, Y.R. and Scarlett, C.J., 2015. Optimization of far-infrared vacuum drying conditions for miang leaves (camellia sinensis var. assamica) using response surface methodology. Food Science and Biotechnology 24: 461-469.

Horuz, E. and Maskan, M., 2015. Hot air and microwave drying of pomegranate (*Punica granatum* L.) arils. Journal of Food Science and Technology 52: 285-293.

Horuz, E., Bozkurt, H., Karatas, H. and Maskan, M., 2017. Drying kinetics of apricot halves in a microwave-hot air hybrid oven. Heat Mass Transfer 53(6): 2117-2127.

Huang, L.L., Qiao, F. and Fang, C.F., 2015. Studies on the microstructure and quality of iron yam slices during combined freeze drying and microwave vacuum drying. Journal of Food Processing and Preservation 39: 2152-2160.

Jafarifar, M., Chayjan, R.A., Dibagar, N. and Alaei, B., 2017 Modeling some engineering properties of walnut kernel undergoing different drying methods with microwave pretreatment. Quality Assurance and Safety of Crops and Foods 9(4): 463-478.

Jahedi Rad, S., Kaveh, M., Sharabiani, V.R. and Taghinezhad, E., 2018. Fuzzy logic, artificial neural network and mathematical model for prediction of white mulberry drying kinetics. Heat and Mass Transfer 54: 3361-3374.

Kantrong, H., Tansakul, A. and Mittal, G.S., 2014. Drying characteristics and quality of shiitake mushroom undergoing microwave-vacuum drying and microwave-vacuum combined with infrared drying. Journal of Food Science and Technology 51: 3594-3608.

Kaveh, K., Abbaspour-Gilandeh, Y., Amiri Chayjan, R., Taghinezhad, E. and Mohammadigol, R., 2018. Mass transfer, physical, and mechanical characteristics of terebinth fruit (*Pistacia atlantica* L.) under convective infrared microwave drying. Heat and Mass Transfer 54(7): 1879-1899.

Kaveh, M. and Amiri Chayjan, R., 2017. Modeling thin-layer drying of turnip slices under semi-industrial continuous band dryer. Journal of Food Processing and Preservation 41: e12778.

Kaveh, M., Amiri Chayjan, R. and Esna Ashri, M., 2015. Thermal and physical properties modelling of terebinth fruit (*Pistacia atlantica* L.) under solar drying. Research in Agriculture in Engineering 61: 150-161.

Kaveh, M., Amiri Chayjan, R. and Nikbakht, A.M., 2017. Mass transfer characteristics of eggplant slices during length of continuous band dryer. Heat and Mass Transfer 53: 2045-2059.

Kocabiyik, H., Yilmaz, N., Tuncel, N.B., Sumer, S.K. and Buyukcan M.B., 2016. Quality properties, mass transfer characteristics and energy consumption during shortwave infrared radiation drying of tomato. Quality Assurance and Safety of Crops and Foods 8(3): 447-456.

Krishnamurthy, K., Khurana, H.K., Soojin, J., Irudayaraj, J. and Demirci, A., 2008. Infrared heating in food processing: an overview. Comprehensive Reviews in Food Science and Food Safety 7(1): 2-13.

Kurozawa, L.E., Hubinger, M.D. and Park, K.J., 2012. Glass transition phenomenon on shrinkage of papaya during convective drying. Journal of Food Engineering 108: 43-50.

Liu, Y., Miao, S., Wu, J., Liu, J., Yu, H. and Duan, X., 2015. Drying characteristics and modeling of vacuum far-infrared radiation drying of flos lonicerae. Journal of Food Process and Preservation 39: 338-348.

Magalhaes, A.S., Silva, B.M., Pereira, J.A., Andrade, P.B., Valentao, P. and Carvalho, M., 2009. Protective effect of quince (*Cydonia oblonga* Miller) fruit against oxidative hemolysis of human erythrocytes. Food and Chemical Toxicology 47: 1372-1377.

Mohsenin, N.N., 1986. Physical properties of plant and animal materials. Gordon and Breach Science, New York, NY, USA.

Motevali, A., Minaei, S., Khoshtaghaza, M.H. and Amirnejat, H., 2011. Comparison of energy consumption and specific energy requirements of different methods for drying mushroom slices. Energy 36: 6433-6441.

Noshad, M., Mohebbi, M., Shahidi, F. and Mortazavi, S.A., 2012. Multi-objective optimization of osmotic – ultrasonic pretreatments and hot-air drying of quince using response surface methodology. Food and Bioprocess Technology 5: 2098-2110.

Onwude, D.I., Hashim, N., Abdan, K., Janius, R. and Chen, G., 2018. Modelling the mid-infrared drying of sweet potato: kinetics, mass and heat transfer parameters, and energy consumption. Heat and Mass Transfer. https://doi.org/10.1007/s00231-018-2338-y.

Paengkanya, S., Soponronnarit, S. and Nathakaranakule, A., 2015. Application of microwaves for drying of durian chips. Food and Bioproduct Processing 96: 1-11.

Ponkham, K., Meeso, N., Soponronnarit, S. and Siriamornpun, S., 2012. Modeling of combined far-infrared radiation and air drying of a ring shaped-pineapple with/without shrinkage. Food and Bioproduct Processing 90: 155-164.

Reich, G., 2005. Near-infrared spectroscopy and imaging: basic principles and pharmaceutical applications. Advanced Drug Delivery Reviews 57: 1109-1143.

Sakai, N. and Hanzawa, T., 1994. Applications and advances in far-infrared heating in Japan. Trends in Food Science and Technology 5: 357-362.

Salarikia, A., Ashtiani, S.H.M. and Golzarian, M.R., 2017. Comparison of drying characteristics and quality of peppermint leaves using different drying methods. Journal of Food Processing Preservation 41(3): e12930.

Shi, Q., Zheng, A. and Zhao, Y., 2014. Optimization of combined heat pump and microwave drying of yacon (*smallanthus sonchifolius*) using response surface methodology. Journal of Food Processing Preservation 38: 2090-2098.

Silva, B.M., Andrade, P.B., Valentao, P., Ferreres, F., Seabra, R.M. and Ferrira, M.A., 2004. Quince (*Cydonia oblonga* Miller) fruit (pulp, peel, and seed) and jam: antioxidant activity. Journal of Agricultural and Food Chemistry 52: 4405-4712.

Silva, B.M., Valentao, P., Seabra, R.M. and Andrade, P.B., 2008. Quince (*Cydonia oblonga* Miller): an interesting dietary source of bioactive compounds. In: Papadopoulos, K.N. (ed.) Food chemistry research developments. Nova Science Publishers, New York, NY, USA.

Sorouraddin, M.H., Rashidi, M.R., Ghorbani-Kalhor, E. and Asadpour-Zeynali, K., 2005. Simultaneous spectrofluorimetric and spectrophotometric determination of melatoninand pyridoxine in pharmaceutical preparations by multivariate calibration methods. Pharmacology 60: 451-458.

Sumic, Z., Tepic, A., Vidovic, S., Vakula, A., Vladic, J. and Pavlic, B., 2017. Process optimization of chanterelle (*cantharellus cibarius*) mushrooms vacuum drying. Journal of Food Processing Preservation 41(2): e12822.

Wang, H., Zhang, M. and Adhikari, B., 2015. Drying of shiitake mushroom by combining freeze-drying and mid-infrared radiation. Food and Bioproduct Processing 94: 507-517.

Wang, J. and Sheng K., 2006. Far-infrared and microwave drying of peach. LWT – Food Science and Technology 39: 247-255.

Ziaforoughi, A., Yousefi, A.R. and Razavi, S.M.A., 2016. A comparative modeling study of quince infrared drying and evaluation of quality parameters. International Journal of Food Engineering 12(9): 901-910.

Zielinska, M., Sadowski, P. and Blaszczak, W., 2015. Freezing/thawing and microwave-assisted drying of blueberries (*Vaccinium corymbosum* L.). LWT – Food Science and Technology 62: 555-563.